J Neurophysiol 99: 704–717, 2008.
First published December 12, 2007; doi:10.1152/jn.01100.2007.

Responses to Tactile Stimulation in Deep Cerebellar Nucleus Neurons Result From Recurrent Activation in Multiple Pathways

Nathan C. Rowland and Dieter Jaeger
Emory University, Department of Biology, Atlanta, Georgia

Submitted 3 October 2007; accepted in final form 9 December 2007

Rowland NC, Jaeger D. Responses to tactile stimulation in deep cerebellar nucleus neurons result from recurrent activation in multiple pathways. *J Neurophysiol* 99: 704–717, 2008. First published December 12, 2007; doi:10.1152/jn.01100.2007. In a previous study, we found that neurons in the deep cerebellar nuclei (DCN) respond to 5-ms brief facial tactile stimulation in rats anesthetized with ketamine-xylazine with multiphasic response patterns lasting over 200 ms. It remained unclear, however, to what extent these responses were shaped not only by ascending sensory input from the trigeminal nuclei but also by interactions with other major cerebellar afferent systems, in particular the inferior olive (IO) and cerebral cortex. In the present study, we recorded from the IO, cerebral cortex, cerebellar granule cell layer (GCL), and DCN during the presentation of 5-ms facial tactile stimuli to elucidate potential mechanisms of how extended DCN response patterns are generated. We found that tactile stimulation resulted in robust multiphasic local field potentials responses in the IO as well as in the activation of a wide region of the somatosensory cortex (SI) and the primary motor cortex (MI). DCN neurons responded to electrical stimulation of any of these structures (IO, SI, and MI) with complex temporal patterns strikingly similar to air-puff lip stimulation responses. Simultaneous recordings from multiple structures revealed that long-lasting activation patterns elicited in DCN neurons were based on recurrent network activation in particular between the IO and the DCN with a potential contribution of DCN rebound properties. These results are consistent with the hypothesis that sensory stimulation triggers a feedback network activation of cerebellum, IO, and cerebral cortex to generate temporal patterns of activity that may control the timing of behavior.

INTRODUCTION

In the rat, sensory information from the face is conveyed from the trigeminal nuclear complex to the cerebellum through three principal pathways: direct trigeminocerebellar fibers, the inferior olive, and the somatosensory cortex via the basilar pontine nuclei (Waite and Tracey 1995). In a previous study, we demonstrated that stimulation of the orofacial region in anesthetized rats not only activates the cerebellar cortex (Bower and Woolston 1983; Shambes et al. 1978) but also produces reliable strong responses in the deep cerebellar nuclei (DCN) (Rowland and Jaeger 2005). Single units in the DCN responded to 5-ms air-puff stimulation of the lips with multiphasic and extended temporal activity patterns that were mostly invariant to stimulus parameters. These sensory-evoked responses could be described as a combination of three temporal components: a brief excitation comprising one or a few spikes with a mean latency of 10 ± 0.9 (SD) ms, a strong inhibition at a mean latency of 18 ± 1.25 ms, and a second prolonged excitation with a mean latency of 291 ± 13.3 ms. Different combinations and different amplitudes of these response components were present in different neurons, but each neuron showed a stable temporal response pattern. This gave the overall impression that each DCN neuron was tuned to emit a specific response pattern regardless of stimulus condition.

Previous studies have suggested that different components of sensory responses in the DCN result from sequential inputs from the trigeminal nuclei, inferior olive, and cerebral cortex (Armstrong et al. 1973, 1975b; Eccles et al. 1974), although a possible component of postinhibitory rebound was also mentioned (Armstrong et al. 1973). The potential for strong postinhibitory rebounds of DCN neurons was later confirmed in brain slice recordings (Aizenman and Linden 1999).

The simple view of relating each component of DCN sensory responses to a specific input pathway or intrinsic mechanism may be misleading, however. Many potential cellular and systems level mechanisms for interactions and feedback between the contributing systems exist, and the extended time course of DCN responses would clearly allow such responses to be influenced by recurrent loops of processing. Evidence for such interactions between cerebellar, olivary, and cortical processing in the anesthetized rat has previously been suggested by studies examining the influence of olivary activity on Purkinje cell responses to mossy fiber input (Schwarz and Welsh 2001) and cortical influence on sensory responses in the olive (Brown and Bower 2002). Given the dominant input sources to DCN neurons from climbing fibers from the inferior olive (Ruigrok 1997) and mossy fibers from the ascending trigeminal system and the cerebral cortex via the pontine nuclei (Morissette and Bower 1996), we undertook an analysis of the contribution and interaction of these sources in the generation of extended DCN response patterns to sensory stimulation in the ketamine/xylazine-anesthetized rat.

Partial results from this study have been published in abstract form (Rowland and Jaeger 2004).

METHODS

All procedures were approved by the Institutional Animal Care and Use Committee of Emory University and were in accordance with National Institutes of Health guidelines.

Surgery

Thirty-seven male Sprague-Dawley rats (Charles River Laboratories, Wilmington, MA; mean weight = 411 g; mean age = 72 day)

Address for reprint requests and other correspondence: D. Jaeger, Emory University, Dept. of Biology, 1510 Clifton Rd. NE, Atlanta, GA 30322 (E-mail: djaeger@emory.edu).

The costs of publication of this article were defrayed in part by the payment of page charges. The article must therefore be hereby marked "*advertisement*" in accordance with 18 U.S.C. Section 1734 solely to indicate this fact.

were temporarily immobilized with halothane in a large bell jar and then anesthetized with a mixture of ketamine (25 mg/ml), xylazine (1.3 mg/ml), and acepromazine (0.25 mg/ml). A loading dose of 125 mg/kg ketamine was injected intraperitoneally, and thereafter the anesthetic mixture was administered at a rate of 0.5 ml/h using a syringe infusion pump (Stoelting, Wooddale, IL, Model No. 53100). This ensured that the anesthetic level of the animal did not fluctuate on short time scales during the experiment. However, the rate of infusion was manually increased when the animal's foot withdrawal reflex became visible. The rate was decreased when a marked slowdown of the heart rate was observed, which was recorded through two electrocardiographic (EKG) leads placed below the chest wall, digitally displayed and made audible by speaker. The animal was placed in a custom-made stereotaxic frame for the duration of the experiment, with the head fixed pointing downward at a 32° angle relative to horizontal to facilitate access to the cerebellum. The animal's temperature was maintained at 36°C through feedback monitoring using a rectal probe and heating pad. Sterile lubricating ointment (Phoenix Pharmaceutical, St. Joseph, MO, Model No. NDC-57319-760-25) was placed over the animal's eyes to prevent corneal dehydration during the experiment. The scalp was incised, and the muscles overlying the occipital skull were removed before exposing the cerebrum and cerebellum with rongeurs. An acrylic dam was fashioned around the surgical site and filled with warm mineral oil to prevent desiccation of the brain tissue and to provide clear visualization of the brain surface for the remainder of the experiment. Finally, the dura mater overlying the cerebrum and cerebellum was resected immediately before the start of recording.

Recording, inactivation, and electrical stimulation protocols

All local field potential (LFP) recordings were amplified 1,000 times and fast-spike activity was amplified 10,000 times using an AC differential amplifier (A-M Systems, Carlsborg, WA). LFP activity in the inferior olive, cerebral cortex, and granule cell layer (GCL) was low-pass filtered on-line between 0.1 and 500 Hz. Fast spike activity in the DCN was band-pass filtered on-line between 300 Hz and 5 kHz. Recordings were made in reference to a chloridized silver wire implanted subcutaneously behind the skull. All signals were routed through an analog to digital interface before being stored on a PC at a sampling rate of 10 kHz.

Deep cerebellar nuclei

Extracellular recordings (Humphrey and Schmidt 1990) in the deep cerebellar nuclei were performed with glass microelectrodes pulled from capillary glass tubing (World Precision Instruments, Sarasota, FL, Model No. TW120F-3) to a tip diameter of 5–10 μm. Glass electrodes were filled with a solution of 2% Chicago Sky Blue (Sigma-Aldrich, St. Louis, MO, Model No. C-8679) in 0.5 M sodium acetate resulting in a mean impedance of 5 MΩ. They were advanced toward the DCN at an angle of 71° relative to horizontal using a hydraulic microdrive (Narishige International USA, Long Island, NY, Model No. MWS-32). Single units were generally encountered between 3 and 4 mm below the surface of the cerebellar cortex in accordance with the atlas of Paxinos and Watson (1998). At the end of some DCN neuron recordings, 5 μA continuous current with the electrode as positive were used to emit the electrode solution containing Chicago Sky Blue from the tip of the electrode (see Rowland and Jaeger 2005 for details). This typically produced a blue dot measuring 50–150 μm in diameter that remained stable throughout histological processing of the tissue and allowed for postmortem reconstruction of recording sites. Neurons from all three nuclei were recorded, as our previous study showed robust sensory responses containing identical components in all nuclei. However, the majority of recorded neurons were obtained from the interpositus nucleus, which in previous work has been most clearly linked to tactile responses.

Inferior olive

LFP activity in the inferior olive (IO) was recorded with glass microelectrodes as described for DCN recording in the preceding text. The IO was approached from the dorsal brain stem ~0.5–1 mm caudal to the vermal uvula and 0.5 mm lateral to the midline. The electrode was lowered between 3 and 4 mm below the surface of the brain stem at an angle of 65° relative to horizontal. Single units at these coordinates displayed a slow and aperiodic 1- to 3-Hz spiking characteristic of climbing fiber activity. At the end of some recording sessions, we placed a small extracellular deposit of Chicago Sky Blue at the coordinates detailed in the preceding text. Following these sessions, postmortem histological processing was conducted to verify location of the electrode in the rostral dorsal accessory olive. This site was chosen for recording based on the results of studies that show this area to be most responsive to somatosensory input from the face (Gellman et al. 1983, 1985; Weiss et al. 1993). All IO penetrations took place contralaterally from the site of DCN recording.

Inactivation experiments of the IO were carried out by pressure injecting 0.25 μl of 0.2 or 2% muscimol (Sigma M1523) solution at the same coordinates that IO recordings were obtained from. The solution was injected via silica tubing (Polymicro Technologies, Phoenix, AZ, Model No. TSP040105) with an inner diameter of 41 μm and outer diameter of 107 μm, which was glued to a tungsten microelectrode (A-M Systems, Model No. 575300) such that the tubing ended flush with the electrode tip. The muscimol solution was mixed with 2% Chicago Sky Blue to allow histological reconstruction of the injection sites.

Electrical stimulation of the IO was carried out using epoxylite insulated 5 MΩ tungsten microelectrodes (A-M Systems) inserted at the same coordinates that field potential recordings were obtained from. Current was driven through the electrodes using a stimulus isolation unit (SIU) (World Precision Instruments, Model No. A365). Once a DCN neuron responsive to air-puff stimuli to the lip was isolated, 25–50 trials of olivary stimulation were administered. Stimuli were comprised of two 0.1-ms square-wave pulses of opposite polarity separated by 0.1 ms. The current amplitude set on the SIU necessary to elicit responses in these neurons ranged from 50 to 500 μA. For most recordings, trials used for quantitative analyses were obtained with 100 or 200 μA simulation intensity. The stimulus voltage was also monitored, and remained $<$10 V for all stimuli. Effective stimulus voltages ranged between 2 and 8 V. It should be noted that for the brief pulses employed, the set stimulus current was not achieved at the electrode tip due to capacitances in the system, polarization of the electrode tip, and possible shunts into the oscilloscope or other circuits. As with air-puff stimuli, each trial consisted of 1,000 ms of prestimulus activity and 1,500 to 3,000 ms of poststimulus activity.

Cerebral cortex

Tungsten microelectrodes (same as for IO in the preceding text) were used to record LFP activity from the cerebral cortex. During response mapping of the cerebral cortex, recordings took place in a grid with 1-mm spacing in all areas of the dorsal cortex, extending from 4 mm anterior to bregma to 6 mm posterior to bregma rostrocaudally and from 1 to 6 mm lateral to the midline in both hemispheres. The electrode position was monitored by a scale bar in the microscope objective. Individual recording positions in the matrix were bypassed or slightly altered when large surface vessels were encountered at a particular coordinate. Electrodes were lowered to a depth of between 750 and 1,000 μm perpendicularly below the cortical surface where the largest responses to air-puff stimulation of the lip were found. Partial maps of cortical areas to air-puff stimulation of the lip were obtained for 11 animals and pooled to produce a full map. All cerebral cortical penetrations took place contralaterally from the site of DCN recording.

Inactivation of somatosensory cortex was undertaken by injecting 10 μl 2% lidocaine solution at a depth of 2–4 mm over 5 min using a 10-μl Hamilton syringe. Coordinates used were 4–6 mm lateral to the midline and 2 mm anterior to 6 mm posterior to bregma in the hemisphere contralateral to simultaneous DCN recordings (n = 21 animals). These sites were designated as M1 or S1 cortex due to their stereotaxic coordinates following previous mapping studies (Zilles 1985, 1990). Bilateral injections were performed in an additional five animals. We also attempted to inactivate cortex through the mechanism of spreading depression by placing filter paper wetted with a 20% KCl solution on the cortical surface. However, we were unable to succeed in suppressing cortical activity as determined by EEG recordings. This finding is in agreement with an earlier study that ketamine anesthesia prevents the mechanism of cortical spreading depression (Gorelova et al. 1987).

Paired bipolar electrodes were used to electrically stimulate sites in the cerebral cortex. The electrodes were constructed from two epoxylite-coated No. 000 Morpho insect pins (0.25 mm diam; 3.85 mm length) with an intertip distance of 1 mm. The electrodes were placed perpendicularly below the cortical surface at a depth of 1–2 mm, where the largest responses to cortical stimulation in the DCN were found. The criteria for administering the stimuli were the same as for olivary stimulation, i.e., the DCN neuron's prima facie responsiveness to air-puff stimuli. The stimulus source, composition, amplitude, and trial parameters matched those of olivary stimulation.

Cerebellar GCL

Tungsten microelectrodes as described above were lowered perpendicularly 500 μm below the pial surface of folium crus IIa, 3.5–4 mm laterally from the midline of the vermis and in the middle of the folium rostrocaudally. This location corresponds to the granule cell layer of the crown of folium crus IIa (Morissette and Bower 1996). To confirm our location in the GCL, once the electrode was in place, several trials of air-puff stimuli were directed at the animal's ipsilateral upper lip to check for evoked negative deflections of the LFP trace in accordance with results from our previous study (Rowland and Jaeger 2005). Once a responsive area of the GCL was identified, the electrode was left in this position for the remainder of the experiment. All GCL penetrations took place ipsilaterally from the site of DCN recording.

Histology

At the end of each experiment, animals were given a lethal dose of Nembutal (125 mg/kg) ip. The absence of all deep reflexes was verified before performing a transcardial perfusion with 60 ml of 0.01 M potassium phosphate buffered saline followed by 60 ml of 15% sucrose in 10% phosphate-buffered formalin. The brain was then removed from the skull and placed in this same solution for 24 h, followed by a 30% sucrose in 10% phosphate-buffered formalin solution for an additional 24 h. After thorough fixation, the brain was sectioned in 50-μm slices using a Reichert-Jung Kryostat (Leica Microsystems, Bannockburn, IL, Model No. 2800 Frigocut-E). Post-fixed slices were serially incubated in distilled H_2O for the duration of sectioning. Slices were then serially mounted onto slides and allowed to dry for 24 h.

When present, the Chicago Sky Blue stains were apparent in fresh tissue. However, a mild cresyl violet counterstain was applied to enhance the boundaries of the structure of interest, i.e., the IO and/or the deep cerebellar nuclei. Digital images of slices with blue dots were taken. In the case of the DCN, individual electrode tracks were manually reconstructed by reconciling the position of the blue dot inside the nuclei with electrode coordinates described during recording. Recordings were performed in all three deep cerebellar nuclei; however, the majority took place in the interposed nuclei, as these are the predominant target of the rostral dorsal accessory olive (Buisseret-Delmas 1988). Given technical experience gained through our previous study (Rowland and Jaeger 2005), the relationship between the electrode coordinates described during recording and the final position of the blue dot inside the deep cerebellar nuclei were consistent enough to rely solely on the coordinates to indicate the targeted nucleus in most experiments.

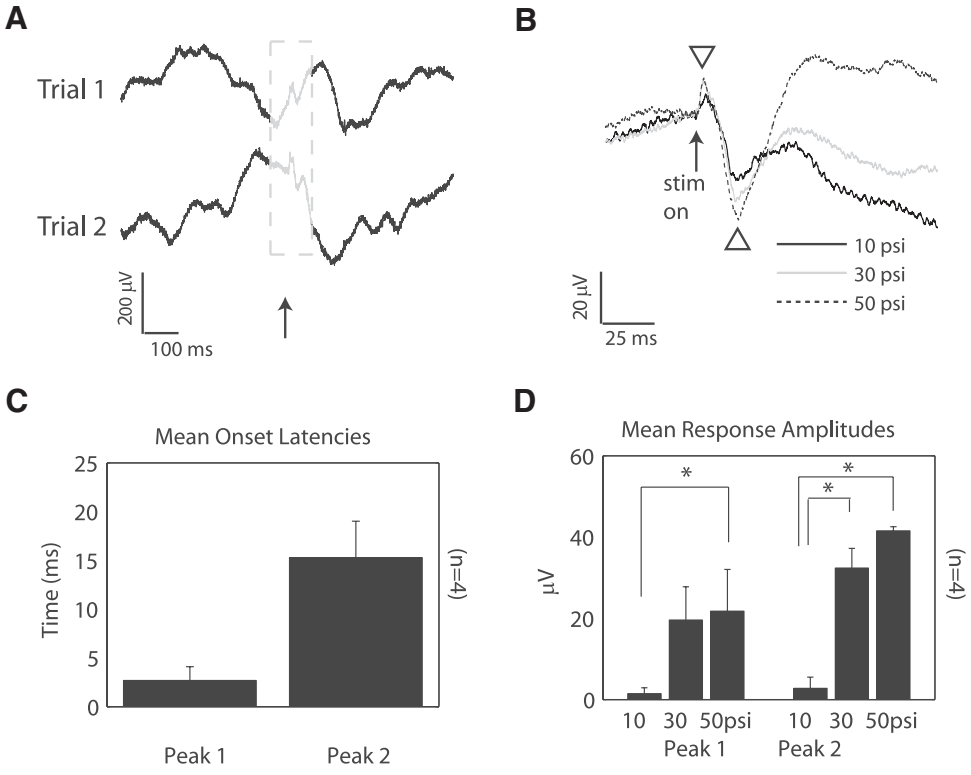

FIG. 1. Inferior olive (IO) responses to air-puff stimulation of the lip. *A*: 2 single traces of local field potential (LFP) activity from IO recordings are shown, in which air-puff stimulation occurs at a different phase of the spontaneous oscillation. In both traces, responses to air-puff stimulation consist of a sharp positive deflection that is followed by a protracted and more robust negative deflection. *B*: averaged IO LFP activity in response to 3 different air-puff intensities is shown for a different animal. ↑, time of air-puff delivery to the lip. △, ▽, positive and negative peaks in the LFP response. *C*: the mean onset of the 1st (2.68 ± 1.4 ms) and 2nd peak times (15.3 ± 3.7 ms) for mean IO LFP traces displaying a significant response are shown (n = 4 animals, air-puff intensity = 30 psi). *D*: increase in LFP response amplitude with increasing air-puff stimulus amplitude. *, significant differences (Kruskal Wallis test, peak 1; ANOVA, peak 2).

All chemicals were obtained from Fisher Scientific or Sigma Chemical unless otherwise noted.

Air-puff stimulation

Once a DCN single unit was isolated during recording, several trials of air-puff stimuli directed at the upper lip ipsilateral to the DCN recording were administered to check for responses in the neuron. The time delay between triggering of the air-puff device and actual delivery of air to the face was measured at 5 ms (see Rowland and Jaeger 2005 for details). This value has been subtracted from onset latency values reported in RESULTS. DCN responses to air-puff stimulation were provisionally determined by observing an absence of spiking immediately following the stimulus using superimposed spike train activity on an oscilloscope and/or an on-line spike discrimination and peri-event histogram algorithm. Inhibition was observed to be the most consistent response component generated by air puffs to the body of anesthetized rats in our previous study (Rowland and Jaeger 2005). If no response was observed, the neuron was abandoned in search of other neurons responsive to the stimulus. Once a responsive neuron was identified, 50 trials of air-puff stimuli were presented. Each trial consisted of 1,000 ms of prestimulus activity followed by the presentation of the air puff and 1,500–3,000 ms of additional poststimulus activity.

Data analysis

All data were analyzed using MATLAB 7 (R14; MathWorks, Natick, MA).

LFP activity

All LFP traces from a particular recording site and stimulus type were averaged into a mean trace. LFP responses in the cerebral cortex typically consisted of a brief, single, monophasic negative deflection of the signal following the stimulus. Therefore only the first 100 ms of poststimulus activity was evaluated because all responses in the data set were completed by this time. The 100 ms prior to the stimulus was averaged as the baseline mean, and only traces that fell 3 SD below this baseline mean were evaluated for a response. To eliminate random, nonstimulus locked excursions below the threshold, the additional conditions of the trace falling below the threshold within the first 25 ms following the stimulus, the trace remaining below the threshold for $\geq$10 ms and the trace returning to the threshold were implemented. Traces not meeting these conditions were excluded from latency analyses and were assigned a peak amplitude of zero.

In addition to an evoked negative deflection, LFP responses in the IO displayed an initial positive deflection. The onset of this initial response was determined by finding the start of the maximum positive-going segment in the trace after discarding the first millisecond of poststimulus data containing the stimulation artifact. Because the responses in IO LFP were typically longer lasting than in cortex, 170 ms of poststimulus activity were evaluated with the 50 ms preceding the stimulus averaged as the baseline mean. Scoring the baseline only for a short segment preceding stimulation was implemented to avoid highly variable baseline readings due to ongoing IO LFP oscillations. Traces with IO LFP responses that fell 3 SD below the mean within the first 30 ms following the stimulus were scored as responsive and were used for the quantitative evaluation of response components.

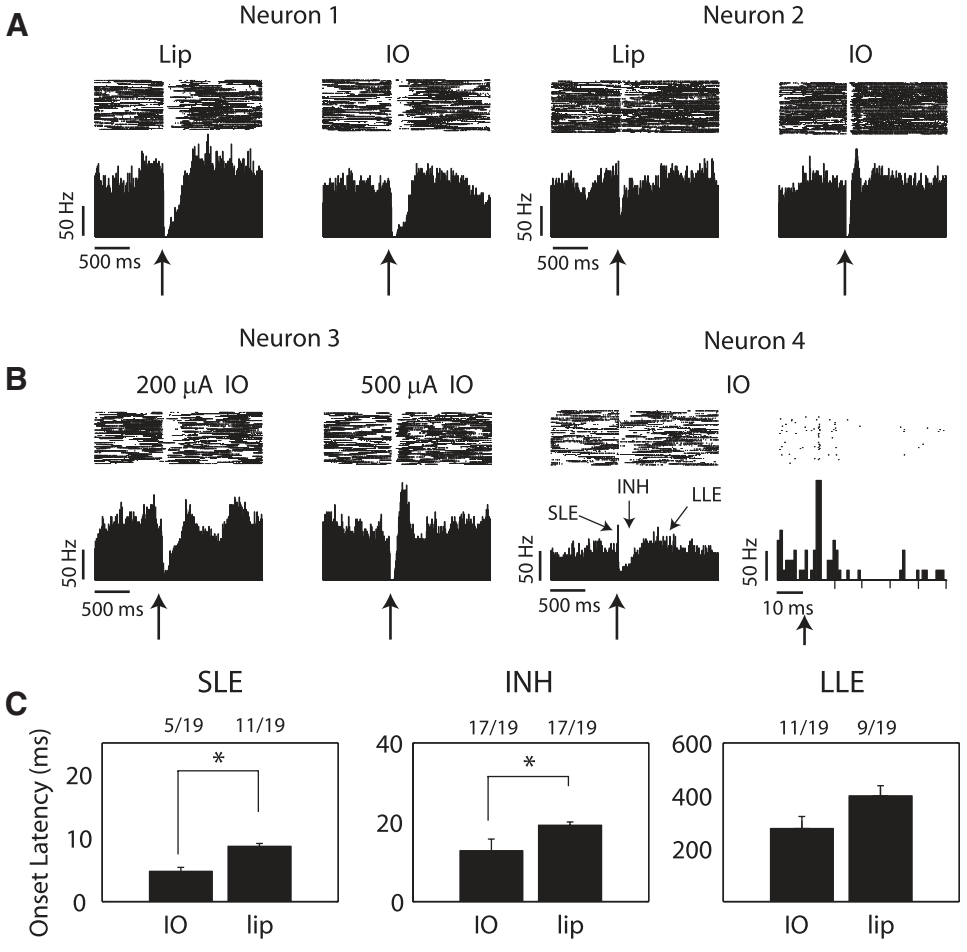

FIG. 2. Deep cerebellar nuclei (DCN) neuron responses to electrical stimulation of the IO. *A*: peri-event histograms and raster plots of DCN neurons responding to air-puff stimulation of the lip and electrical stimulation of the IO are shown. *Neuron 1* responds with an inhibition of the same latency and duration to each stimulus. In addition to a brief inhibition, *neuron 2* responds with a sharp long-latency excitation to IO stimulation not seen with air-puff lip stimulation. *B*: DCN neuron responses to IO stimulation at 2 different stimulation strengths are shown for *neuron 3*. Electrical stimulation of the IO at 500 μA produces a short inhibition and strikingly robust long-latency excitation, a feature not present with the 200-μA stimulation level. A robust short-latency excitation is observed in n*euron 4* (time scale zoomed for *neuron 4* in *right-hand panel*). Overall, DCN neurons displayed all 3 responses components to IO stimulation—short-latency excitation, inhibition, and long-latency excitation—as for lip stimulation. All histograms were constructed with 5-ms bin width. *C*: comparison of the mean onset latencies of response components in DCN neurons (n = 13 animals and 19 neurons) to both IO and lip stimulation. With the exception of the onset of the short-latency excitation and inhibition, which begin at a significantly shorter latency than the air-puff lip response ($P < 0.05$, Wilcoxon rank sum test), all other measures of response components were similar between the 2 stimulus types. In the analysis, the lowest IO stimulation amplitude that produced a DCN response was used. SLE, short-latency excitation; INH, inhibition; LLE, long-latency excitation.

Spike activity

Individual DCN neuron spike times were discriminated from background activity using a window discrimination method (see Rowland and Jaeger 2005 for details). In recordings involving olivary or cortical stimulation, spike trains were often contaminated with stimulus artifacts, which led to the exclusion of a short time window for spike train analysis. Individual spike times were subsequently convolved with a Gaussian kernel to produce an analog representation of instantaneous spike rate (Paulin 1996; Rowland and Jaeger 2005). As in our previous study, DCN responses to both air-puff and electrical stimulation produced three primary response components: a short- and long- latency excitation as well as a strong intervening inhibition. These response components were identified and parameterized for each neuron with a computer algorithm using significant deviations in the instantaneous spike rate from the baseline period (see Rowland and Jaeger 2005 for details).

In all recordings, DCN neurons were tested with air-puff stimuli first. The order of the remaining stimulation of the IO and cerebral cortex was chosen arbitrarily. Stimulation of all three sites occurred in separate blocks of trials except in a few experiments where they were randomly intermixed. All data were subjected to analyses of variance to determine significant differences between groups. Data that did not meet the criteria for normality and equal variance among groups were analyzed with nonparametric equivalents to the *t*-test (Wilcoxon rank sum) and one-way ANOVA (Kruskal Wallis). The Lilliefors test, a modified version of the Kolmogorov-Smirnov test, was used to test for normality. This analysis is not dependent on the prespecification of the mean and variance. Levene's test was used to test for equality of variance among groups. Again, this test does not presume normally distributed data. Standard parametric tests (*t*-test, ANOVA, etc.) were used for data meeting normality and equal variance criteria. Tukey-kramer's post hoc test was used to identify significantly different groups. All values are reported in means ± SE unless otherwise indicated.

RESULTS

IO LFPs showed robust biphasic responses to lip stimulation

Olivary neurons have previously been found to show low-threshold responses to mechanical stimulation of the face and direct trigeminal nerve stimulation in the urethane anesthetized rat (Cook and Wiesendanger 1976). Receptive fields were reported to cover 20–50% of the contralateral face. We recorded LFP activity in the IO (see METHODS) in ketamine–xylazine-anesthetized rats with contralateral air-puff stimulation to the face to determine the timing relationship between olivary activation and DCN responses in the same preparation (Rowland and Jaeger 2005).

Using air-puff stimuli to the contralateral upper lip, a biphasic, positive-then-negative deflection was elicited in single trials of IO LFP activity (Fig. 1*A*). Reliable responses could be elicited at all phases of the ongoing olivary oscillation. In four animals, we analyzed the relation between air-puff intensity and IO LFP responses. The stimulus intensity of 10 psi was near threshold of triggering a response in most cases (Fig. 1*D*), but by 30 psi, a significantly larger ($P < 0.05$, ANOVA) response was elicited, which increased little for a further stimulus increase to 50 psi (Fig. 1*D*). This relationship was true for both peaks of the LFP response and is quite similar to the increase in DCN neuron spike responses with increasing stimulation amplitude (Rowland and Jaeger 2005). At 30 psi, the early small positive deflection in the IO LFP response began at a mean latency of 2.68 ± 1.4 (SD) ms ($n = 4$ animals) and corresponded most likely to activation of an afferent fiber volley. At the same stimulus intensity, the larger negative IO LFP component had a mean onset latency of 15.3 ± 3.7 ms ($n = 4$ animals; Fig. 1*C*). This component most likely corresponds to postsynaptic depolarization which can trigger spike responses in the IO (see DISCUSSION).

DCN neuron temporal responses to electrical stimulation of the IO and air-puff lip stimulation did not differ

Electrical stimulation of the olive while recording in the DCN has been performed in previous studies (Armstrong et al. 1973; Eccles et al. 1974; Kitai et al. 1977; Ruigrok 1997). These studies show good agreement on evoking a sequence of fast excitation, inhibition, and delayed excitation in DCN neurons with IO stimulation. Here we wished to determine the temporal response patterns of DCN neurons to IO microstimulation with a focus on how these responses compared with those from the cerebral cortex and peripheral stimulation of the lip in the same DCN neurons. The main result from this comparison was that electrical stimulation of the IO produced complex response patterns remarkably similar to lip stimulation in the same DCN neurons. Overall, 17 of 19 DCN neurons recorded [($n = 13$ animals, 15 neurons in interposed nuclei (IN), 2 neurons in medial nucleus (MN), 2 neurons in lateral nucleus (LN)] responded to electrical stimulation of the IO. Eleven of the 17 responsive neurons displayed a qualitatively similar response pattern to IO stimulation as the same neuron's response to air-puff stimulation of the lip (Fig. 2*A, neuron 1,* IN), whereas 6 neurons showed different responses to the two stimuli (Fig. 2A*, neuron 2*, IN). Increasing the IO stimulus strength significantly altered the late excitation of the temporal response pattern in two of five neurons (Fig. 2*B, neuron 3,* LN). This grading of the long-latency excitation in particular was also seen in previous studies (Armstrong et al. 1973;

FIG. 3. Cerebral cortical responses to air-puff stimulation of the lip. *A*: single traces of LFP activity from cerebral cortical (SI) recordings are shown. *Top*: regular rhythm; *bottom*: more mixed frequencies. Nevertheless, a sharp negative deflection in response to the lip stimulus is clearly discernible in both traces. *B*: several individual traces of LFP activity from cerebral cortical (SI) recordings are shown superimposed. In each case, the peak of the response occurs ~25–30 ms after the stimulus (gray vertical bars 5 ms apart). ↑, air-puff onset. *C*: a depth profile of cortical (SI) responses to lip stimulation is shown. Each response is composed of a mean of 20 traces. Responses were recorded from 400 μm to 2 mm below the cortical surface at SI. The response is most robust between 1,200 and 1,600 μm below the cortex; however, a significant response persists in deeper cortical layers as well. Figure 2, *A–C,* are taken from activity recorded in the same animal. This depth profile was seen in 5 recording sites in S1 and M1 and in another animal. *D*: Average LFP responses to lip stimulation at various cortical coordinates in a different animal are shown from 2 mm anterior to bregma to 6 mm posterior to bregma (laterality = 6 mm from midline). Each response is composed of a mean of 25 traces. Responses generally increase in amplitude in a rostral (ant) to caudal (pos) direction. Calibration bar = 1 mm. *E*: average peak response amplitudes in a grid of recording sites. Robust responses were obtained in S1, and much weaker ones in M1. The data were pooled from 11 animals, but some sites were stimulated in as few as 3 animals. M1 and S1 are outlined as ovals according to previous maps by Zilles (1985). *F*: mean LFP onset in MI (bregma +2, lateral 4 mm coordinates) and SI (bregma −4, lateral 5 mm) responses to lip are shown. The responses were scored for the 2 of 5 animals where this M1 site showed a response, whereas in S1, 5 of 6 animals showed a response that could be quantitatively analyzed.

Ruigrok 1997). In our population of recorded neurons, however, the long-latency excitation could also decrease with an increasing IO stimulus strength ($n = 3$ of 5 neurons). Overall, IO stimulation elicited all response components seen with lip stimulation, including a short-latency excitation (Fig. 2B, neu*ron 4,* IN, zoomed in right panel), which was seen in 5 of 19 neurons. The mean onset of both the short-latency excitatory and inhibitory DCN neuron responses to IO stimulation were significantly earlier than that of lip stimulation; however, the amplitude and duration of each of the response components were statistically the same between IO and lip stimulation with no apparent differences among the nuclei. A detailed analysis

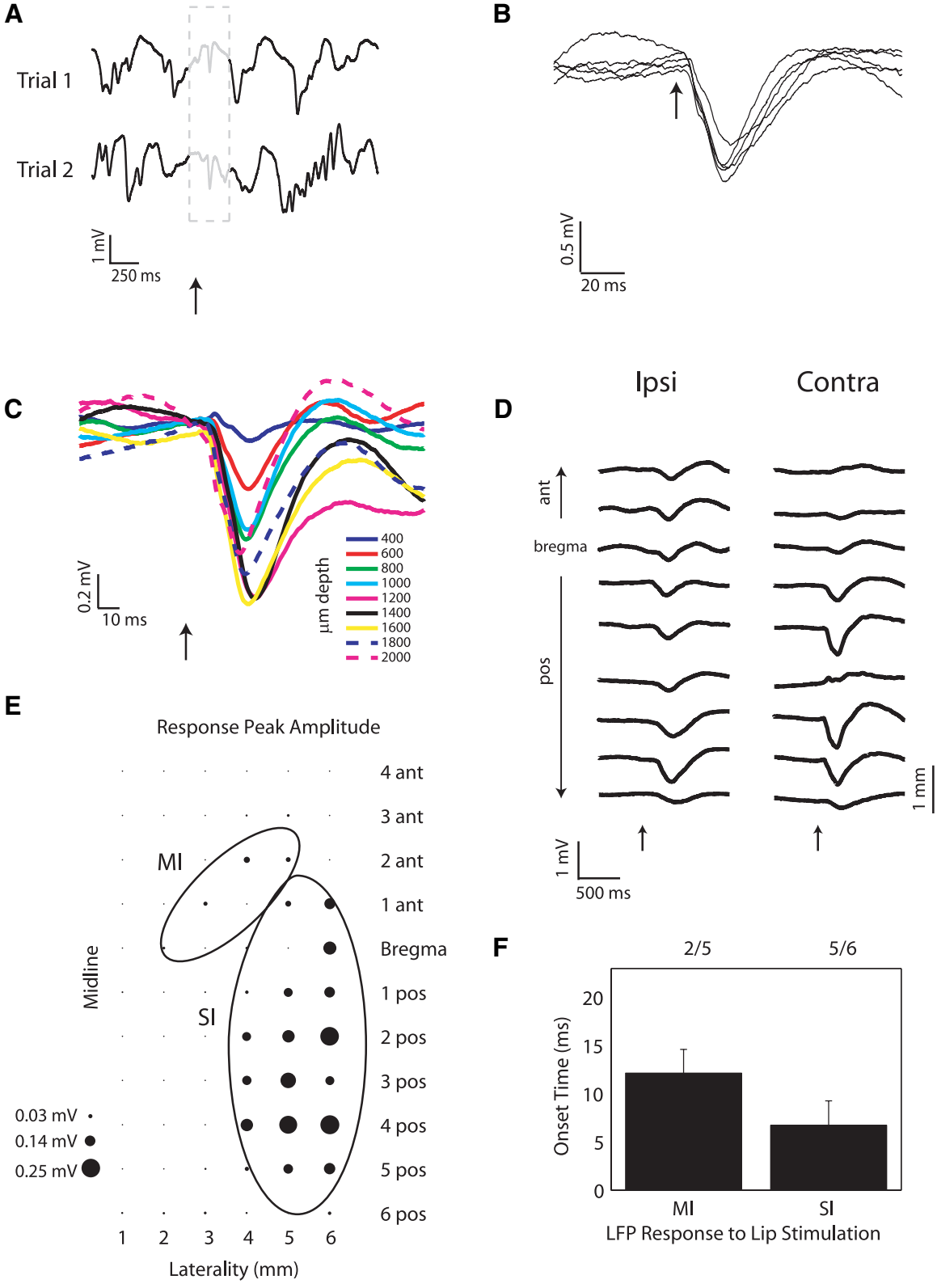

of potential differences between nuclei was not possible with our small sample of MN and LN neurons. We did not aim to perform such a comparison because our previous study with a larger N for lip stimulation alone did not reveal any differences between nuclei (Rowland and Jaeger 2005).

Inactivation of olive shuts down DCN spiking

To determine the contribution of the IO to lip responses, we inactivated the IO with an injection of muscimol (see METHODS) while holding a well-discriminated DCN single-neuron recording ($n = 7$ neurons from 5 animals, all from IN). Shortly after muscimol injection, four neurons stopped spiking. Spiking slowly recovered 30–60 min later, so the cessation of spiking was not due to losing the unit on injection. One other neuron showed a marked slowdown in activity, while the remaining two showed no change in activity. However, during histology, a blue dot indicative of successful Chicago Sky blue labeling could not be recovered in the animals where injection failed to affect DCN firing, and it is likely that a successful muscimol injection was not achieved due to technical reasons like clogged silica tubing. The result of complete cessation of DCN firing following IO inactivation has been previously observed (Benedetti et al. 1983). It is most likely mediated by a pronounced increase of Purkinje cell spiking in the absence of climbing fiber input (Bengtsson et al. 2004). Unfortunately, this result did not allow us to classify detailed lip response components mediated by IO activity.

Lip stimulation activated a wide area of the face representation in the somatosensory cortex

Because air-puff stimuli to the face activate trigeminothalamo-cortical pathways and, furthermore, substantial connections exist between the cerebrum and cerebellum (Allen and Tsukahara 1974), we hypothesized that the DCN neuron sensory responses found in our previous study (Rowland and Jaeger 2005) likely involve a cortical component. However, it was not clear from our initial study which regions of the cortex are involved in this pathway or which components of responses in the deep cerebellar nuclei specifically depend on cortical input. We therefore recorded field potentials in a wide region of the cerebral cortex to determine the areas receptive to air-puff stimulation of the lip. Air-puff stimuli directed at the upper lip predominantly elicited a negative deflection in single trials of the cerebral cortical LFP (Fig. 3*A*). Most of the responses displayed a monophasic profile, with a mean onset at 13.87 ± 2.3 ms ($n = 11$ animals) and a mean peak at 35.03 ± 3.5 ms ($n = 11$ animals, Fig. 3*B*). The response to lip stimulation could be recorded throughout multiple layers of the somatosensory cortex, as shown by the depth profile in Fig. 3*C*, and showed a maximum amplitude at a depth of 1,600 μm. Furthermore, the response deflection of the signal bore the same timing in all layers. We found that air-puff stimulation of the lip could elicit cortical responses in both hemispheres and along a rostrocaudal extent spanning several millimeters (Fig. 3*D*). Our overall plot of the dorsal cortex confirmed the more fine-grained mapping of Zilles (1985) in that lip responses in our recordings were confined to the face area of the somatosensory cortex (Fig. 3*E,* compare with Zilles Fig. 47). We found activation in both the upper and lower lip areas as well as the furry buccal pad, lower jaw, and nose representations (Chapin and Lin 1984; Fig. 3). The vibrissal region also showed clear responses, which may be due to the brief deflection of whiskers following skin indentation of the face (Rowland and Jaeger 2005). MI was also slightly activated (Fig. 3*E,* see coordinates 2 ant/4 lat, 1 ant/3 lat and bregma/2 lat and compare Zilles Fig. 47), with an onset latency delayed by 5 ms on average compared with S1 activation. This increase in delay did not reach significance ($P = 2.8$, Wilcoxon rank-sum test) in our small sample, however.

Inactivation of somatosensory cortex leads to changes in DCN activity

We injected lidocaine into contralateral S1 ($n = 21$ animals) to inactivate this area of cortex (see METHODS) and successfully recorded from 27 DCN neurons (20 IN, 4 MN, 3 LN) before and after cortical lidocaine injection in these animals (lidocaine injections for two different neurons in one animal were performed at intervals >1 h). We found that for nine neurons, spontaneous firing slowed substantially after cortical lidocaine injection (mean spike rate decrease 27 ± 18 Hz corresponding to a 78 ± 17% reduction of baseline firing). In five neurons, we found that the response to lip stimulation was changed. The typical change consisted of an increase in the duration and depth of inhibition (supplemental Fig. S1[1]). In three neurons, this increase in inhibition seemed to be caused by the removal of an excitatory response component because previous to lidocaine injection an inhibitory period was seen on both sides of an intervening excitation (supplemental Fig. S1). This interpretation is supported by the presence of a distinct excitatory peak intervening in the inhibitory response following electrical stimulation of S1 (see Fig. 5). An additional five animals were injected bilaterally, and eight neurons were recorded. A reduction of spiking following injection was observed in two neurons, and overall the effect of bilateral injections did not seem to enhance the resulting

[1] The online version of this article contains supplemental data.

FIG. 4. DCN neuron responses to electrical stimulation of the cerebral cortex. *A*: peri-event histograms of DCN neuron spike activity in response to electrical stimulation of the ipsi- and contralateral S1 (*neuron 1*) and M1 (*neuron 2*) are shown. LFP activity from the simultaneously recorded granule cell layer in crus IIa is shown below each corresponding peri-stimulus histogram (note different time scale). The recordings shown are from 2 different animals. *B*: peri-event histograms showing responses of DCN neurons to contralateral cortical stimulation in a grid with 1-mm spacing [for both *neurons 3* and *4,* MI, primary motor cortex; MI(J), jaw area of primary motor cortex; SI, primary somatosensory cortex; FL, forelimb sensorimotor area; HL, hindlimb sensorimotor area (Zilles 1985)]. The most robust responses were observed in response to stimulation of the M1 (rostromedial) cortex. Stimulation of more caudal areas produces weaker response types with changing response components in the same neuron. Large negative granule cell layer (GCL) LFP deflections were also predominant for rostral cortical stimulation sites. *C*: responses to 30 psi ipsilateral air-puff lip stimulation of corresponding neurons shown in *A* and *B* for cortical stimulation. All histograms were constructed with 5-ms bin width. *D*: mean response amplitudes for all 3 response components comparing stimulation of MI, SI, and lip. Amplitudes represent percentage change from baseline mean spike rate. Proportions above each bar represent significant responses out of the total number tested. *, significant differences ($P < 0.05$, Kruskal-Wallis test).

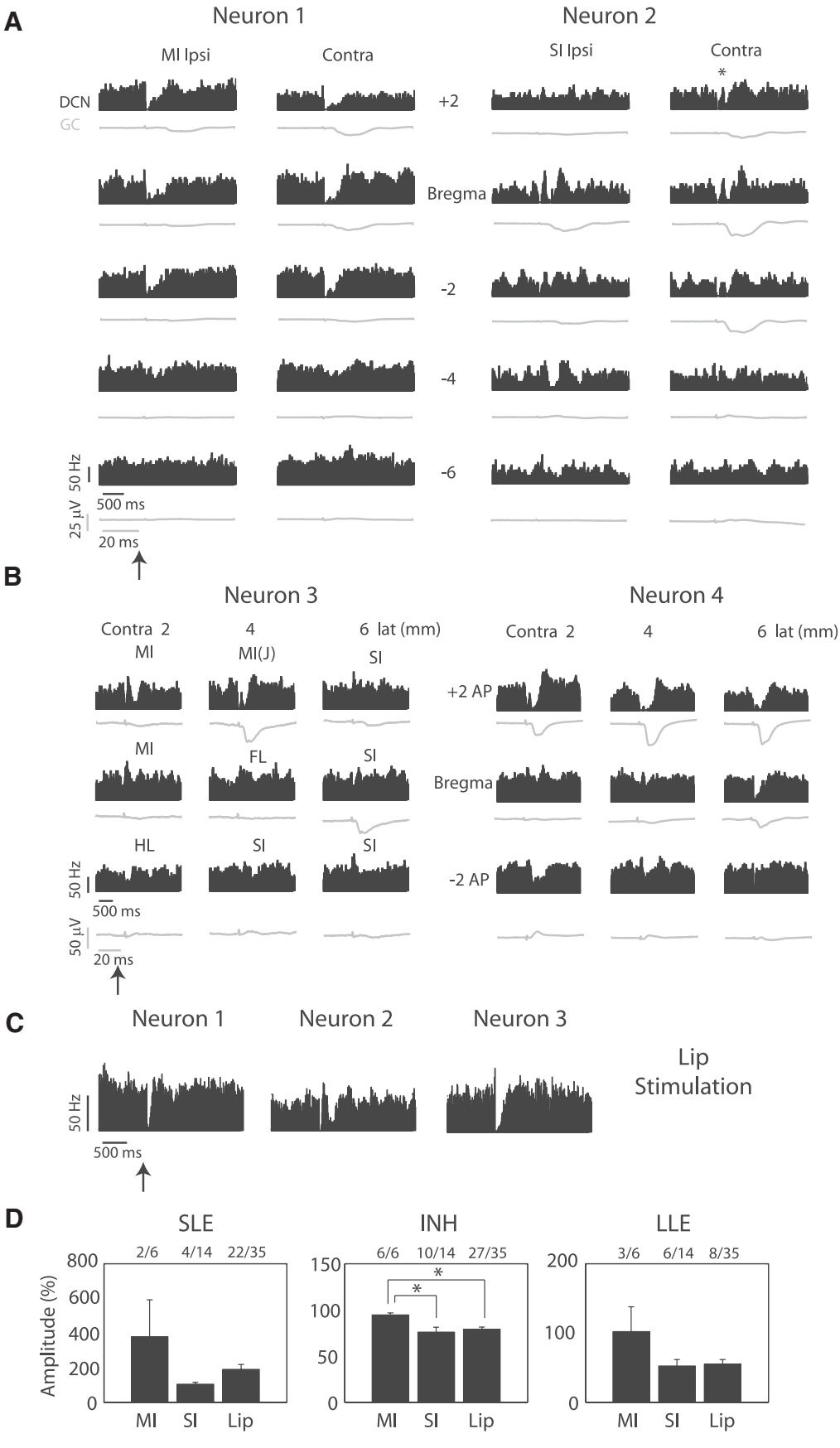
A
Neuron 1
Neuron 2
MI Ipsi
Contra
SI Ipsi
Contra
DCN
GC
+2
Bregma
-2
-4
-6
50 Hz
500 ms
25 µV
20 ms
B
Neuron 3
Neuron 4
Contra 2
4
6 lat (mm)
MI
MI(J)
SI
FL
HL
+2 AP
Bregma
-2 AP
50 Hz
500 ms
50 µV
20 ms
C
Neuron 1
Neuron 2
Neuron 3
Lip
Stimulation
50 Hz
500 ms
D
SLE
INH
LLE
2/6
4/14
22/35
6/6
10/14
27/35
3/6
6/14
8/35
Amplitude (%)
MI
SI
Lip

modest changes in DCN activity. Comparing the limited data of MN and LN neurons available to the IN data, no differences between the nuclei were apparent.

DCN neurons responded to electrical stimulation of both motor and sensory cortical areas

Because of the strong connection from the cerebral cortex to the cerebellum via the pontine nuclei, we were interested in determining the potential contribution of cortical activation to lip stimulation responses in the DCN. A previous study in primates showed that electrical stimulation of either the motor or sensory cortex reliably evokes multiphasic spike response patterns in interpositus neurons (Allen et al. 1977). We were also able to elicit strong responses in DCN spiking in most cases (27 of 37 neurons recorded in 24 animals, 21 IN, 6 MN, 10 LN) when we electrically stimulated contralateral M1 or S1 in the anesthetized rat with single pulse stimuli (see METHODS). Strong responses were elicited both from M1 and S1 sites in the same animals (11 neurons in 7 animals) although the response strength tended to diminish toward caudal areas of S1 (Fig. 4, *A, B,* and *D*). Responses from ipsilateral or contralateral S1 stimulation sites were of nearly equal strength for seven of nine tested neurons with any response [Fig. 4*A, neuron 1* (LN), *neuron 2* (IN)], while the remaining two showed stronger responses with contralateral stimulation. For M1 stimulation, five of seven responsive neurons tested with stimulation in both hemispheres showed greater responses to contralateral stimulation, one showed equal responses, and one showed a bigger ipsilateral response. These data indicate that somatosensory cortex from both hemispheres has nearly equal influence on DCN neurons, while a pronounced laterality is seen in M1. In most neurons, inhibition was the most commonly observed response component (Fig. 4*D*), but excitatory responses could also be elicited from contra- and ipsilateral S1 and M1 stimulation sites in recordings from all nuclei. In contrast to peripheral lip stimulation, which produced responses in single DCN neurons that were relatively invariant to stimulus location (Rowland and Jaeger 2005), electrical stimulation of the cortex could generate responses in single DCN neurons that showed significantly different response components and durations depending which site in cortex was stimulated [Fig. 4*B, neuron 3* (LN), *neuron 4* (IN)]. These responses to cortical stimulation could exceed the strength and duration of lip-stimulation responses in the same neurons (Fig. 4*C*). Given the large area of activated cortex following lip stimulation (Fig. 3) this suggests that *trans*-cortical pathways likely provide major components to DCN lip-stimulation responses and could influence the shape of observed temporal response profiles.

Single DCN neurons integrated input from both the IO and somatosensory cortex

In a subset of 17 neurons (13 IN, 2 MN, 2 LN) from 12 animals, we obtained complete trial sets (50 trials each) for air-puff lip as well as electrical IO and cortical stimulation to compare temporal response patterns for input from all three sites. In a subset of these neurons, all three stimulation sites resulted in similar response patterns [Fig. 5*A, neuron 1* (IN), $n = 3/17$ neurons recorded in 12 animals], but in most neurons, responses to cortical stimulation resulted in a different temporal activation pattern [Fig. 5*A, neuron 2* (IN), $n = 14/17$]. In particular, responses to cortical stimulation frequently produced an excitation which bisected an ongoing inhibitory response (Fig. 5*A, neuron 1* and *2,* $n = 4/8$ neurons with inhibitory responses). Electrical S1 stimulation thus seems to activate inputs to the DCN that are not part of the lip response network.

Feedback interactions between DCN, IO, and cortex with single site stimulation

The DCN responses to IO and cortical stimulation could be primarily due to activation of the direct input pathways from these structures. However, feedback connections between these and other structures could also lead to reentrant network activation of which DCN activity could be an integral part. To test for the possibility of enduring network activity throughout the DCN response patterns to single shock stimulation, we recorded from the IO and DCN while stimulating in cortex (Fig. 6) and from the cortex and DCN while stimulating the IO (Fig. 7). Most interestingly, single 0.1-ms shock activation of S1 or M1 cortical sites ($n = 3$ animals) led to a strong extended response pattern in the IO LFP, which closely paralleled the DCN spike activity (Fig. 6, both neurons from IN). In one animal in particular, this activation extended beyond the usual late excitation and appeared to consist of a dampened network oscillation following S1 stimulation (compare Fig. 6*B*). When stimulating in the IO ($n = 4$ animals), a cortical response was also observed in parallel to DCN responses (Fig. 7, both neurons from IN). In fact, not only the DCN but also the cortical response to IO stimulation was remarkably similar to the result of air-puff stimulation (Fig. 7*A*). In this case, reverberatory components were not observed, and the dominant outcome in the DCN was strong inhibition. These results indicate that indeed the observed extended DCN response patterns with lip or electrical IO or cortical stimulation are embedded in an equally extended activation of an olivary-cerebellar-cortical network.

DISCUSSION

The deep cerebellar nuclei play a critical role in cerebellar function as they provide the only output pathway of cerebellar processing. In the DCN, inhibition from Purkinje cells provides the majority of synaptic input, which is integrated with excitatory input from mossy and climbing fiber collaterals before reaching cerebellar targets primarily in the red nucleus, thalamus, and the IO. Surprisingly for a structure with activity clearly related to motor tasks (van Kan et al. 1993), strong sensory responses with similar features in anesthetized and awake animals are also present in the DCN (Armstrong et al. 1973, 1975b; Eccles et al. 1974). In a previous study, we examined sensory responses in the rat to cutaneous lip stimulation more closely (Rowland and Jaeger 2005), and found that even 5-ms brief stimuli resulted in extended response patterns with distinct components of early excitation, inhibition, and late excitation. The temporal profile of the responses was quite variable between neurons but was not strongly influenced by stimulus location, stimulus intensity, or stimulus duration (Rowland and Jaeger 2005). This lack of sensory information

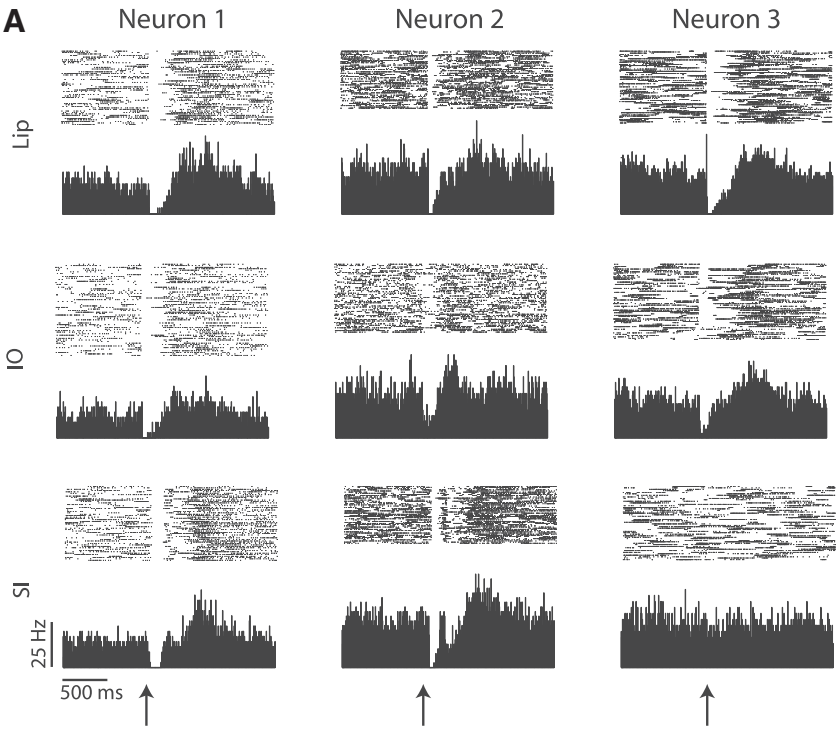

FIG. 5. The integration of cortical and olivary input by DCN neurons. *A*: *neuron 1*, peri-event histogram and raster plot from a single unit in the DCN responding to stimulation of the upper lip with an air-puff and direct electrical stimulation of the IO or somatosensory cortex are shown. The neuron in this example displays very similar response profiles to all 3 stimulus types with a slight additional excitation following S1 stimulation; *neuron 2,* electrical stimulation of the cerebral cortex produces a stronger transient excitation that bisects the ongoing inhibition in this neuron. This feature is not present following stimulation of the lip or IO; *neuron 3,* the neuron in this example is responsive to both stimulation of the lip and the IO but not cortical stimulation. Stimulus onset occurred at ↑. All somatosensory cortical stimulation amplitudes are 1 mA. Stimulation strengths for the IO are: 200 μA (*neurons 1* and *2*) and 1 mA (neuron 3). All histograms were constructed with 5-ms bin width. *B*: summary of LFP response latencies to air-puff stimulation of the lip in IO, SI and spike responses in DCN. Travel time through tubing (5 ms) has been subtracted for all values.

B

Structure	Earliest response to air puff
IO	2.68 ± 1.4 ms
SI	6.74 ± 1.1 ms
DCN	10.0 ± 0.9 ms

in DCN responses led us to hypothesize that sensory stimulation acts as a trigger for DCN neurons to produce invariant temporal activity patterns that might be useful in the temporal control of behavior thought to take place in the cerebellum (Ivry et al. 2002; Mauk et al. 2000).

Control of early excitation, inhibition, and late excitation in DCN sensory responses through multiple feedback pathways

The major finding of the present study examining the pathways involved in generating the temporal patterns in DCN responses to lip stimulation was that both cerebral cortex and the IO are part of a feedback network controlling the extended time course of DCN activation. This is in contrast to earlier descriptions of sensory responses in the DCN, which focused on identifying individual pathways for each particular response component of DCN neurons (Allen et al. 1977; Armstrong et al. 1973; Eccles et al. 1974; Kitai et al. 1977; Ruigrok 1997). Our results indicate that only the fast excitation occurring at around 10 ms following lip stimulation should be ascribed to an ascending sensory pathway. This response component is most likely due to the activation of mossy fibers originating in the trigeminal nuclei and making direct excitatory synapses on DCN neurons (Mantle-St John and Tracey 1987; Marfurt and Rajchert 1991; Phelan and Falls 1991; Somana et al. 1980; Watson and Switzer 1978). A contribution of the IO to fast excitatory responses in the DCN seems unlikely as multiple studies have found that spike responses to tactile stimulation in the IO have latencies well above 15 ms (Brown and Bower 2001; Gellman et al. 1985). Thus despite the short-latency spike response of DCN neurons to electrical stimulation in the IO that we and others (Kitai et al. 1977; Ruigrok 1997) have found, this pathway is overall too slow to account for fast excitatory responses to tactile stimulation. Although we have found a small positive peak in the IO at a short latency of 3 ms following tactile stimulation, this peak likely corresponds to an input fiber volley that does not trigger spikes. Postsynaptic depolarization and spiking in contrast are likely the process underlying the much more pronounced negative peak in the IO LFP at the appropriate latency of 25 ms. Despite the relatively simple feed forward pathways leading to fast excitation in the DCN, these responses could still be shaped by ongoing feedback interactions in the cerebellar-olivary-cortical system. In particular, previous studies have found that stimulation of the red nucleus suppresses sensory responses in the trigeminal nuclei (Davis and Dostrovsky 1986) as well as in the IO (Horn et al. 1998). As the red nucleus receives major input pathways from the DCN and from motor cortex, ongoing activa-

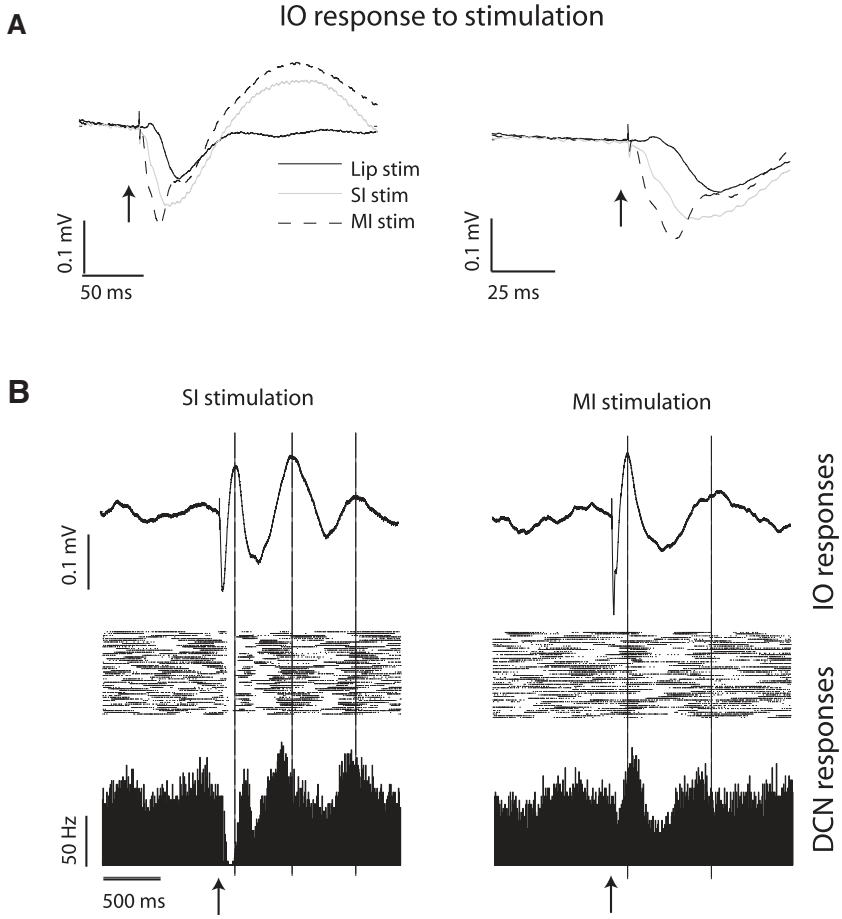

FIG. 6. *A*: 3 traces of mean LFP activation of the IO are shown superimposed (expanded time scale shown in *right panel*). Each trace represents the average of 50 single trials of air-puff stimulation at the lip or electrical stimulation in cortex. *B*: traces of mean IO LFP activation in response to SI (*left*) and MI (*right*) stimulation are shown above simultaneously recorded DCN single neuron activity, represented as peri-stimulus time (PST) histograms. The vertical dashed lines denote the correspondence between IO LFP peaks and single unit responses in the DCN. All panels depict activity recorded in a single animal. [Cortical stimulation strength = 2 mA (8 V); cortical stimulation depth = 2 mm; lip stimulation strength and duration = 30 psi and 5 ms.] Stimulus onset occurred at arrows. All histograms were constructed with 5-ms bin width.

tion of the cerebellar-cortical system could thus shape fast excitatory responses to sensory input.

The inhibitory response to lip stimulation was generally the most robust response component (17 of 19 DCN neurons) but had a highly variable duration. Interestingly, in each neuron tested, IO stimulation resulted in a similar period of inhibition as lip stimulation. The latency of the IO triggered inhibition was 10 ms shorter than the lip stimulation latency and activation of the IO could thus account for the major pathway mediating inhibition following lip stimulation. As synchronous olivary spiking strongly activates populations of Purkinje cells (Welsh et al. 1995) that inhibit neurons in the DCN, this is a plausible pathway. Nevertheless it was quite surprising to see the full amount of inhibition seen with lip stimulation also induced by IO stimulation as a major additional source of inhibition could also derive from Purkinje cell activation driven by mossy fiber input. In fact, strong inhibition was also frequently observed following cortical stimulation, which activated mossy fibers originating from the pontine nuclei (Mock et al. 2006; Morissette and Bower 1996). However, a strong multiphasic LFP activation of the IO was also observed after cortical stimulation, and the time course of this activation closely paralleled inhibitory and excitatory DCN responses. The most direct cortical influence on the IO is most likely mediated by the red nucleus, which receives cortical input and projects to the IO (Oka 1988). Overall our results showing strong DCN inhibition with IO and cortical stimulation in conjunction with the extensive activation of both structures following lip stimulation indicate that the inhibitory response to lip stimulation is mediated jointly by multiple pathways that furthermore strongly interacted with each other.

Finally, a highly variable response component to lip stimulation was given by late excitation, which like inhibition could also be elicited with electrical stimulation in the IO and the cortex. This response could be partly due to rebound spiking following inhibition (Aizenman and Linden 1999). However, in our in vivo data, late excitation was not always preceded by strong inhibition, and strong inhibition was not always followed by late excitation. Thus intrinsic rebound behavior may shape late excitatory responses, but additional network input generally controls this response component. An association of this response component with IO discharge has been previously described (Armstrong et al. 1975a), which is also supported by the observed reduction of Purkinje cell simple spike firing following a complex spike (Schwarz and Welsh 2001; Simpson et al. 1996) that would disinhibit DCN neurons. In some cases, we observed evidence for reverberatory olivocerebellar loop activation as an oscillatory IO field potential with matching modulation of DCN neurons was observed (Fig. 6). A feedback connection between the DCN and the IO that can lead to IO synchronization and oscillation has been previously suggested (Ruigrok 1997; Schwarz and Welsh 2001).

DCN neuron temporal pattern generator hypothesis

Multiple lines of investigation have implicated the cerebellum in the fine temporal control of behavior, be it for the sake of adaptive reflex timing (Medina and Mauk 2000; Medina

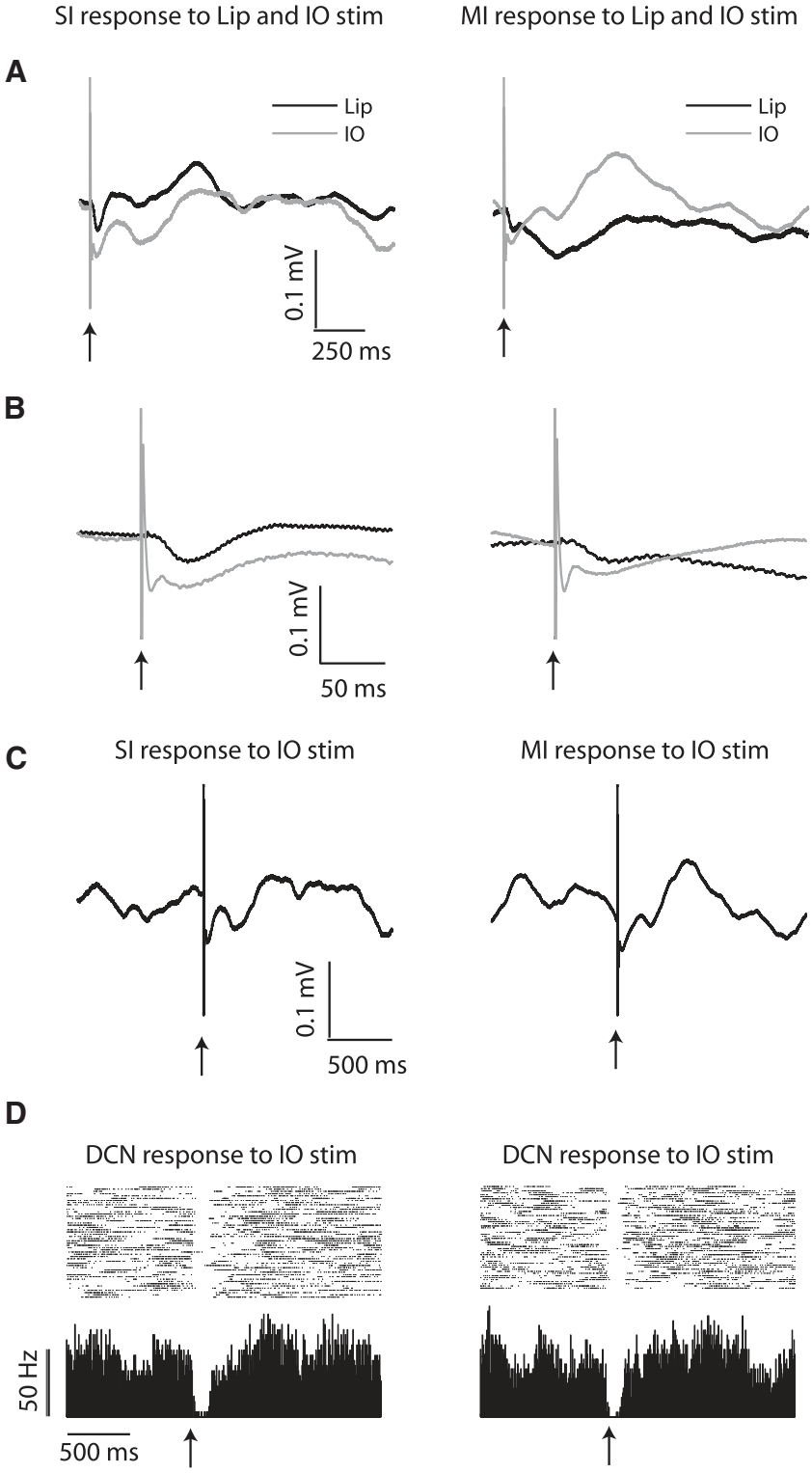

FIG. 7. *A* and *B*: 2 traces of mean LFP activity of cortex (SI and MI) following lip or IO stimulation (expanded time scale shown in *B*). Each trace represents the average of 50 single trials of air-puff stimulation at the lip or electrical stimulation in the IO with a single biphasic pulse. *C* and *D*: LFP activity in response to IO stimulation (*top*) and simultaneously recorded DCN activity, represented as PST histograms (*bottom*). All panels depict activity recorded in a single animal. [IO stimulation strength = 1 mA (7 V); lip stimulation strength and duration = 30 psi and 5 ms.] Stimulus onset occurred at ↑. All histograms were constructed with 5-ms bin width.

et al. 2000), timing of motor sequences such as reaching-grasping (van Kan et al. 1994) or throwing (Martin et al. 1996), coordination of behavior directed at sensory data gathering (Bower 1997), or even cognitive timing mechanisms (Ivry 1997). Any timing mechanism the cerebellum is executing would need to be reflected in the timing of output activity of particular populations of DCN neurons. Our previous study of extended temporal responses to sensory input in DCN neurons found that the time course of these responses does not code for sensory information, which is in agreement with the hypothesis that the time course of this activity reflects the temporal control of behavior. In the present study, we followed up on the question by which circuit the temporal patterns of DCN neurons are generated. One possibility previously suggested is that temporal patterns are generated purely by interactions between cerebellar cortex and the DCN and are shaped by cerebellar

cortical plasticity (Medina et al. 2000; Raymond et al. 1996). Our present data demonstrating a very close association between IO activity and extended DCN sensory responses support the alternative notion that the strong feedback loop between the cerebellum and the IO is intimately involved with temporal pattern generation in DCN neurons (Ruigrok 1997; Schwarz and Welsh 2001). We found that widespread areas of cortex also have an influence on this activation but that no particular cortical area is needed in the generation of extended DCN response patterns to sensory input. To be adaptive in behavior, the olivo-cerebellar generation of temporal patterns clearly needs to be shaped by learning. Although the classic cerebellar learning theory has focused on the climbing-fiber-induced parallel fiber depression on Purkinje cells (LTD), our evidence for widespread feedback loop activation underlying DCN activity patterns in combination with emerging evidence for plasticity mechanisms at many stages of these loop pathways including the DCN themselves (Aizenman et al. 1998; Hansel et al. 2001) as well as the GCL (Gall et al. 2005) suggests that cerebellar learning is far more distributed and complex than the classic Marr-Albus theory (Albus 1971; Marr 1969) accounts for. To unravel this complexity, simultaneous recordings in awake animals from multiple structures in these loop pathways in combination with stimulation and inactivation approaches will be needed.

ACKNOWLEDGMENTS

We thank B. Buffalo, R. Calabrese, F. Gordon, M. Mustari, and K. Sathian for helpful comments. We especially thank C. Gunay and D. Kurzyniec for technical support.

GRANTS

This work was supported by National Institutes of Health Grants RO1 MH-065634, and F31 GM-020685.

REFERENCES

Aizenman CD, Linden DJ. Regulation of the rebound depolarization and spontaneous firing patterns of deep nuclear neurons in slices of rat cerebellum. *J Neurophysiol* 82: 1697–1709, 1999.

Aizenman CD, Manis PB, Linden DJ. Polarity of long-term synaptic gain change is related to postsynaptic spike firing at a cerebellar inhibitory synapse. *Neuron* 21: 827–835, 1998.

Albus JS. A theory of cerebellar function. *Math Biosci* 10: 25–61, 1971.

Allen GI, Gilbert PF, Marini R, Schultz W, Yin TC. Integration of cerebral and peripheral inputs by interpositus neurons in monkey. *Exp Brain Res* 27: 81–99, 1977.

Allen GI, Tsukahara N. Cerebrocerebellar communication systems. *Physiol Rev* 54: 957–1006, 1974.

Armstrong DM, Cogdell B, Harvey RJ. Effects of afferent volleys from the limbs on the discharge patterns of interpositus neurons in cats anaesthetized with alpha-chloralose. *J Physiol* 248: 489–517, 1975a.

Armstrong DM, Cogdell B, Harvey RJ. Responses of interpositus neurons to nerve stimulation in chloralose anesthetized cats. *Brain Res* 55: 461–466, 1973.

Armstrong DM, Cogdell B, Harvey RJ. Responses of interpositus neurons to stimulation of forelimb cutaneous afferents in chloralose-anesthetized cats. *J Physiol* 245: 28P–29P, 1975b.

Benedetti F, Montarolo PG, Strata P, Tempia F. Inferior olive inactivation decreases the excitability of the intracerebellar and lateral vestibular nuclei in the rat. *J Physiol* 340: 195–208, 1983.

Bengtsson F, Svensson P, Hesslow G. Feedback control of Purkinje cell activity by the cerebello-olivary pathway. *Eur J Neurosci* 20: 2999–3005, 2004.

Bower JM. Control of sensory data acquisition. *Int Rev Neurobiol* 41: 489–513, 1997.

Bower JM, Woolston DC. Congruence of spatial organization of tactile projections to granule cell and Purkinje cell layers of cerebellar hemispheres of the albino rat: vertical organization of cerebellar cortex. *J Neurophysiol* 49: 745–766, 1983.

Brown IE, Bower JM. Congruence of mossy fiber and climbing fiber tactile projections in the lateral hemispheres of the rat cerebellum. *J Comp Neurol* 429: 59–70, 2001.

Brown IE, Bower JM. The influence of somatosensory cortex on climbing fiber responses in the lateral hemispheres of the rat cerebellum after peripheral tactile stimulation. *J Neurosci* 22: 6819–6829, 2002.

Buisseret-Delmas C. Sagittal organization of the olivocerebellonuclear pathway in the rat. II. Connections with the nucleus interpositus. *Neurosci Res* 5: 494–512, 1988.

Chapin JK, Lin CS. Mapping the body representation in the SI cortex of anesthetized and awake rats. *J Comp Neurol* 229: 199–213, 1984.

Cook JR, Wiesendanger M. Input from trigeminal cutaneous afferents to neurones of the inferior olive in rats. *Exp Brain Res* 26: 193–202, 1976.

Davis KD, Dostrovsky JO. Modulatory influences of red nucleus stimulation on the somatosensory responses of cat trigeminal subnucleus oralis neurons. *Exp Neurol* 91: 80–101, 1986.

Eccles JC, Sabah NH, Taborikova H. The pathways responsible for excitation and inhibition of fastigial neurones. *Exp Brain Res* 19: 78–99, 1974.

Gall D, Prestori F, Sola E, D'Errico A, Roussel C, Forti L, Rossi P, D'Angelo E. Intracellular calcium regulation by burst discharge determines bidirectional long-term synaptic plasticity at the cerebellum input stage. *J Neurosci* 25: 4813–4822, 2005.

Gellman R, Gibson AR, Houk JC. Inferior olivary neurons in the awake cat: detection of contact and passive body displacement. *J Neurophysiol* 54: 40–60, 1985.

Gellman R, Houk JC, Gibson AR. Somatosensory properties of the inferior olive of the cat. *J Comp Neurol* 215: 228–243, 1983.

Gorelova NA, Koroleva VI, Amemori T, Pavlik V, Bures J. Ketamine blockade of cortical spreading depression in rats. *Electroencephalogr Clin Neurophysiol* 66: 440–447, 1987.

Hansel C, Linden DJ, D'Angelo E. Beyond parallel fiber LTD: the diversity of synaptic and non-synaptic plasticity in the cerebellum. *Nat Neurosci* 4: 467–475, 2001.

Horn KM, Hamm TM, Gibson AR. Red nucleus stimulation inhibits within the inferior olive. *J Neurophysiol* 80: 3127–3136, 1998.

Humphrey DR, Schmidt EM. Extracellular single-unit recording methods. In: *Neurophysiological Techniques. II. Applications to Neural Systems*, edited by Boulton AA, Baker GB, Vanderwolf CH. Clifton, NJ: Humana, 1990, p. 1–64.

Ivry R. Cerebellar timing systems. *Int Rev Neurobiol* 41: 555–573, 1997.

Ivry RB, Spencer RM, Zelaznik HN, Diedrichsen J. The cerebellum and event timing. *Ann NY Acad Sci* 978: 302–317, 2002.

Kitai ST, McCrea RA, Preston RJ, Bishop GA. Electrophysiological and horseradish peroxidase studies of precerebellar afferents to the nucleus interpositus anterior. I. Climbing fiber system. *Brain Res* 122: 197–214, 1977.

Mantle-St John LA, Tracey DJ. Somatosensory nuclei in the brain stem of the rat: independent projections to the thalamus and cerebellum. *J Comp Neurol* 255: 259–271, 1987.

Marfurt CF, Rajchert DM. Trigeminal primary afferent projections to "non-trigeminal" areas of the rat central nervous system. *J Comp Neurol* 303: 489–511, 1991.

Marr D. A theory of cerebellar cortex. *J Physiol* 202: 437–470, 1969.

Martin TA, Keating JG, Goodkin HP, Bastian AJ, Thach WT. Throwing while looking through prisms. I. Focal olivocerebellar lesions impair adaptation. *Brain* 119: 1183–1198, 1996.

Mauk MD, Medina JF, Nores WL, Ohyama T. Cerebellar function: coordination, learning or timing? *Curr Biol* 10: R522–525, 2000.

Medina JF, Garcia KS, Nores WL, Taylor NM, Mauk MD. Timing mechanisms in the cerebellum: testing predictions of a large-scale computer simulation. *J Neurosci* 20: 5516–5525, 2000.

Medina JF, Mauk MD. Computer simulation of cerebellar information processing. *Nat Neurosci , Suppl* 3: 1205–1211, 2000.

Mock M, Butovas S, Schwarz C. Functional unity of the ponto-cerebellum: evidence that intrapontine communication is mediated by a reciprocal loop with the cerebellar nuclei. *J Neurophysiol* 95: 3414–3425, 2006.

Morissette J, Bower JM. Contribution of somatosensory cortex to responses in the rat cerebellar granule cell layer following peripheral tactile stimulation. *Exp Brain Res* 109: 240–250, 1996.

Oka H. Functional organization of the parvocellular red nucleus in the cat. *Behav Brain Res* 28: 233–240, 1988.

Paulin MG. System identification of spiking sensory neurons using realistically constrained nonlinear time series models. In: *Advances in Processing and*

Pattern Analysis of Biological Signals, edited by Gath I, Inbar G. San Diego, CA: Academic, 1996, p. 183–194.

Paxinos G, Watson C. *The Rat Brain in Stereotaxic Coordinates.* 1998. New York: Plenum,

Phelan KD, Falls WM. A comparison of the distribution and morphology of thalamic, cerebellar and spinal projection neurons in rat trigeminal nucleus interpolaris. *Neuroscience* 40: 497–511, 1991.

Raymond JL, Lisberger SG, Mauk MD. The cerebellum: a neuronal learning machine? *Science* 272: 1126–1131, 1996.

Rowland C, Jaeger D. Cutaneous responses in the deep cerebellar nuclei of ketamine-anesthetized rats are shaped by a strong contribution from the somatosensory cortex. *Soc Neurosci Abstr* 536.16, 2004.

Rowland NC, Jaeger D. Coding of tactile response properties in the rat deep cerebellar nuclei. *J Neurophysiol* 94: 1236–1251, 2005.

Ruigrok TJ. Cerebellar nuclei: the olivary connection. *Prog Brain Res* 114: 167–192, 1997.

Schwarz C, Welsh JP. Dynamic modulation of mossy fiber system throughput by inferior olive synchrony: a multielectrode study of cerebellar cortex activated by motor cortex. *J Neurophysiol* 86: 2489–2504, 2001.

Shambes GM, Gibson JM, Welker W. Fractured somatotopy in granule cell tactile areas of rat cerebellar hemispheres revealed by micromapping. *Brain Behav Evol* 15: 94–140, 1978.

Simpson JI, Wylie DR, DeZeeuw CI. On climbing fiber signals and their consequence(s). *Behav Brain Sci* 19: 384–398, 1996.

Somana R, Kotchabhakdi N, Walberg F. Cerebellar afferents from the trigeminal sensory nuclei in the cat. *Exp Brain Res* 38: 57–64, 1980.

van Kan PLE, Horn KM, Gibson AR. The importance of hand use to discharge of interpositus neurons of the monkey. *J Physiol* 480: 171–190, 1994.

van Kan PL, Houk JC, Gibson AR. Output organization of intermediate cerebellum of the monkey. *J Neurophysiol* 69: 57–73, 1993.

Waite PME, Tracey DJ. Trigeminal sensory system. In: *The Rat Nervous System* (2nd ed.), edited by Paxinos G. San Diego, CA: Academic, 1995, p. 705–724.

Watson CRR, Switzer IRC. Trigemingal projections to cerebellar tactile areas in the rat-origin mainly from n. interpolaris and n. principalis. *Neurosci Lett* 10: 77–82, 1978.

Weiss C, Disterhoft JF, Gibson AR, Houk JC. Receptive fields of single cells from the face zone of the cat rostral dorsal accessory olive. *Brain Res* 605: 207–213, 1993.

Welsh JP, Lang EJ, Suglhara I, Llinas R. Dynamic organization of motor control within the olivocerebellar system. *Nature* 374: 453–457, 1995.

Zilles K. Anatomy of the neocortex: cytoarchitecture and myeloarchitecture. In: *The Cerebral Cortex of the Rat*, edited by Kolb B, Tees RC. Cambridge, MA: MIT, 1990, p. 77–112.

Zilles K. *The Cortex of the Rat: A Stereotaxic Atlas.* New York: Springer-Verlag, 1985.